Received: 11 November 2019 | Revised: 5 February 2020 | Accepted: 11 February 2020

DOI: 10.1002/aic.16947

PROCESS SYSTEMS ENGINEERING

AIChE JOURNAL

Renewable production of ammonia and nitric acid

Ganzhou Wang[1] | Alexander Mitsos[1,2,3] | Wolfgang Marquardt[1]

[1]RWTH Aachen University, Process Systems Engineering, Aachen, Germany

[2]JARA-ENERGY, Jülich, Germany

[3]Institute of Energy and Climate Research—Energy Systems Engineering (IEK-10), Forschungszentrum Jülich GmbH, Jülich, Germany

Correspondence
Wolfgang Marquardt, RWTH Aachen University, Process Systems Engineering, 52056 Aachen, Germany.
Email: w.marquardt@fz-juelich.de

Funding information
Bosch-Forschungsstiftung

Abstract

Decarbonization of the power sector offers ammonia industry an opportunity to reduce its CO_2 emissions through sector coupling. Extending from our previous work, we propose a power-based process for ammonia and nitric acid production. The coupling of nitric acid production facilitates highly efficient heat integration between steam electrolysis and the rest of the process. We investigate the economic performance of the production complex through a model-based dynamic optimization approach, considering scenarios with or without incorporation of intermittent wind power as well as deployment of battery storage. In all cases, the wind power integration proves to be economic with a peak-to-base load ratio of up to 2.3. The new process reduces primary energy consumption by more than 13% compared to conventional technologies. However, it is only economically competitive with help of either a low-cost battery storage or a higher carbon price on fossil fuels. The results also confirm the importance of considering process dynamics during process design.

KEYWORDS

dynamic optimization, electrification, Haber-Bosch, process design, sustainability

1 | INTRODUCTION

The rapidly growing share of renewable power generation offers manufacturers opportunities to reduce their carbon dioxide emissions by electrification.[1,2] Within the chemical industry, various molecules and their electrochemical production routes are being investigated.[3] Through sector coupling and flexible operation, industrial processes are capable of providing ancillary services in power markets.[4,5] Thus, they can act as large-scale buffers to help increase capability of the electricity grid to incorporate renewables.[6,7]

Today's ammonia production exhibits a high carbon footprint,[8] thus motivating research on sustainable production methods.[9,10] Electrified ammonia production dates back to the 1920s, where the Haber-Bosch process was coupled with a large-scale hydro-powered alkaline water electrolysis.[11] This two-step synthesis route remains a promising option.[9] Research works on this option can be grouped on unit operations, processes and supply chains: (a) on the unit operation level, Cheema and Krewer[12] use steady-state simulations to demonstrate a wide operating range of a three-bed autothermic Haber-Bosch reactor system. Reese et al.[13] show technical feasibility of a lab-scale Haber-Bosch process driven by intermittent wind power. Millet,[14] Petipas et al.[15] and Mougin[16] investigate transient operability of electrolyzers, such as proton exchange membrane (PEM) electrolyzer[14] and solid oxide electrolyzer (SOE),[15,16] and report no additional degradation on the stack level; (b) on the process level, we[17] propose an ammonia-based energy storage process involving the usage of a reversible high-temperature solid-oxide fuel cell. Chen et al.[18] present a novel design of an ammonia synthesis system for a solar thermochemical energy storage system. The new design enables direct production of supercritical steam up to 650°C. Demirhan et al.[10] apply a superstructure framework to optimally configure and dimension ammonia production processes based on renewable resources and investigate the options of PEM and alkaline electrolyzers. Allman et al.[19,20] propose to embed operation information into a design problem in order to estimate

operating costs under power dynamics; (c) on the supply chain level, recent works analyze the potential of incorporating distributed wind/solar-powered ammonia plants in the countrywide fertilizer industry.[21-23] Economic advantages have been identified in regions with strong ammonia demand and high availability of wind power.

Investigation on heat integration of renewable ammonia production is rare. Our previous work[17] shows that conducting heat integration between a Haber-Bosch process and a high-temperature SOE drastically enhances efficiency. Furthermore, few publications consider process dynamics and their influence on design, especially when intermittent renewables are considered as feeds. The integration of process dynamics helps account for losses of operating efficiency and hence improves the accuracy of cost estimation, as we for instance showed for concentrated solar power.[24] With the explicit consideration of plant controllers, the flexibility of the designed process can be evaluated in a more realistic way.[25]

We propose a power-based acid production complex for ammonia and nitric acid. Heat integration between Haber-Bosch process, SOE, and nitric acid production improves the efficiency as well as the stack utilization of the electrolyzer. We analyze the economic performance of this process through dynamic optimization under variable power inputs as well as different operation strategies. In the following, we first briefly describe the process concept and the models used for the analysis. Next, we introduce case studies and the associated optimization problem formulations. Finally, we present the results of the cases studies and analyze the impacts.

2 | PROCESS DESIGN

As shown in Figure 1a, an ammonia production process is obtained from modification of the closed-loop ammonia-based energy storage process from our previous work.[17] In the following, we will denote this as the *standard concept*. The exothermic ammonia synthesis drives steam generation through the heat exchanger HE-1. The SOE is operated above the thermoneutral voltage (i.e., in the exothermic mode) in order to raise up the temperature of the product stream. This enables the upstream heat exchange in HE-2/3.

Based on the standard concept, we extend the renewable ammonia production with coproduction of nitric acid, see Figure 1b. While the coproduction is common industrial practice, it has not been considered for power-based concepts and here, it serves a special purpose. Namely, a part of the high-temperature heat released from the ammonia burner, which is the first stage of the nitric acid production process, is used for supporting the operation of the SOE through the superheater HE-6. There are several advantages of doing so. First of all, the SOE can be operated in a different operating mode, that is, the thermal-neutral or endothermic mode, with a higher utilization factor of the stack.[26] Hence, the costly investment for the SOE is reduced. Besides this, compared to the case, in which the SOE is operated at the exothermic mode (see e.g., Wang et al.[17]), the size of the superheater is also expected to be smaller because of an increasing temperature difference at both ends. Moreover, the mass flow rate of the hot stream is now available as an additional control degree of freedom for SOE operation. Similar to a standard nitric acid production process (see e.g., Chatterjee and Joshi[27]), the heat exchangers HE-4 and HE-5 are applied to fully make use of the remaining heat. The mutual use of the steam power cycle by both the ammonia and the nitric acid production (HE-1/4/5) is a natural decision based on similar temperature levels. An air separation unit (ASU) is used to produce nitrogen instantly. Even though an installation of a nitrogen storage[28] may help increase the utilization of intermittent power inputs, this option is not considered due to the almost negligible power consumption by the ASU in comparison to that of the hydrogen production. The new

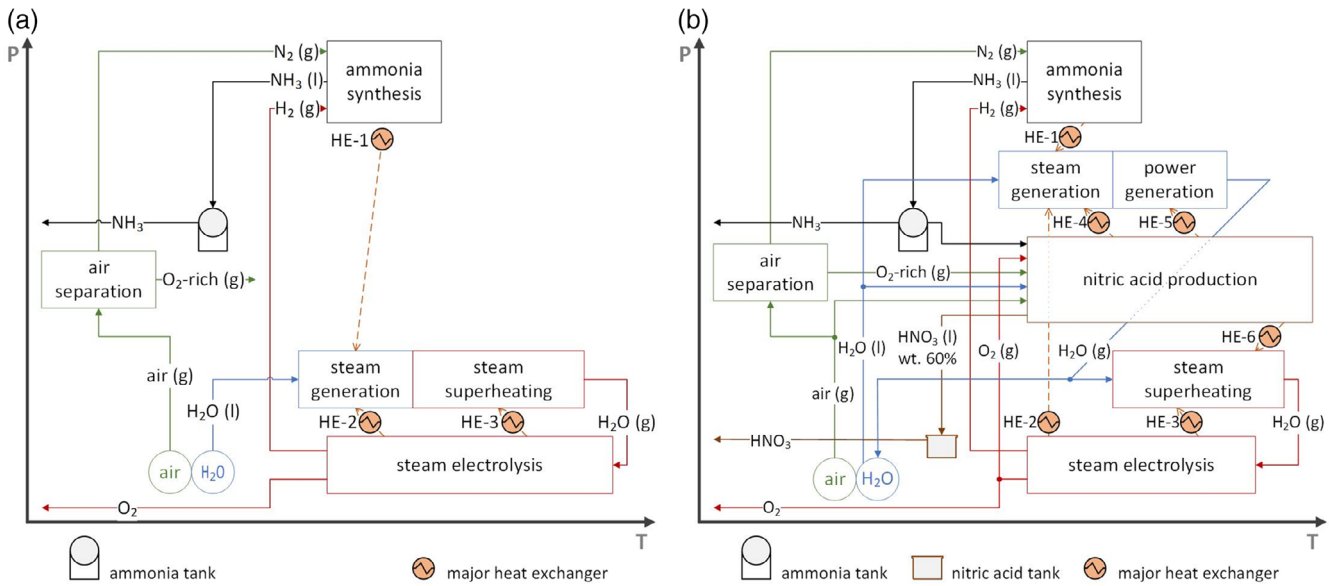

FIGURE 1 Block flow sheets of the process concepts: (a) the standard concept obtained through modifying our previous work[17] and (b) the new concept of a production complex for ammonia and nitric acid [Color figure can be viewed at wileyonlinelibrary.com]

concept utilizes by-products from the ASU. The higher oxygen content of the by-product stream compared to that of the air favors the yield of nitric acid.[27] Within process blocks, heat integration measures are adopted from the literature.[17,27] The detailed process flow sheet is presented in the Supporting Information.

3 | PROCESS MODELING

We dynamically model the production complex based on existing work and first principles. Five submodels are considered: steam generation (STM),[29] steam electrolysis (SOE),[30] air separation (ASU),[31] ammonia synthesis (NH3),[32] and nitric acid production (HNO3).[33,34] We extend our steady-state model[17] to account for relevant process dynamics using dynamic mass and energy balances in units with large inertia: the SOE stacks, the steam boiler, the fixed-bed reactors, the heat exchangers, the cryogenic distillation column, and the absorption column. Quasi-steady-state balance equations are used for all other unit operations. The resulting model consists of 13, 414 model equations with 317 differential states. It is written in gPROMS® and provided at http://permalink.avt.rwth-aachen.de/?id=430437.

4 | CASE STUDY

4.1 | Case definition

An ammonia/nitric production complex built in the north of Germany is studied. We consider three scenarios of the power supply. In the first one, the production complex is operated at steady state at an optimal point with grid electricity. In the second one, the grid power only provides a constant base load. In addition, the production complex absorbs wind power from an optimally sized wind farm. The wind power supply is a product of the installed peak power and a unit wind power curve. The latter is synthesized from historical wind speed data[35] and includes four representative day profiles. The load of the production complex tracks the total power supply dynamically. The last scenario is an extension of the second one. A battery storage is deployed in order to smoothen the dynamics of the power supply due to wind power. The battery has a self-discharging rate and the charging and discharging processes have an equal half-cycle-efficiency. For more information about the synthesis of wind power curve, please refer to the Supporting Information.

In all three scenarios, the specific production cost is minimized while satisfying an emission-reduction target compared to production based on natural gas (NG) of 1.7 t CO_2/t NH_3.[36] By default, the prices of both the grid power and the wind power are based on forecasts in the year 2030,[37,38] and the emission-reduction target is set equal to the amount of emissions from a 500 t/d NG-based plant. A sensitivity analysis on the production cost is carried out. The impact of the plant size is studied within the first scenario. The variation of the power price and the CO_2-footprint of grid power are investigated within the second scenario. Finally, the investment cost of the battery storage is varied to study the economic viability of the third scenario. To estimate the return on investment (RoI), the market prices of ammonia and nitric acid are estimated based on historical values[39,40] and the commodity price outlook.[41] The financial incentives for the CO_2 emission reduction are considered in the framework of the EU Emissions Trading System (ETS), which sets a cap on the maximum level of emissions for heavy energy-using installations and establishes an installation-level market for emission permits.[42] Currently, the European ammonia industry receives nearly full free allowances.[43] The trading of these allowances is assumed to be an extra revenue for the renewable production complex. The technical and economic parameters are released in the Supporting Information.

4.2 | Control scheme

The control scheme serves two purposes: first, the production rate is adjusted so that the power demand of the production complex tracks the power supply and secondly, system states are regulated within the feasible operating range.

For the first purpose, the load tracking is initiated by the SOE because of its high power consumption. The steam feed rate $F_{c/in,E-8}$ of the SOE is adjusted according to

$$\frac{d\dot{F}_{c/in,E-8}}{dt} = \begin{cases} k, & \text{for } \dot{W}_{dmd} < \dot{W}^{set}_{supp}, \\ 0, & \text{for } \dot{W}_{dmd} = \dot{W}^{set}_{supp}, \\ -k, & \text{for } \dot{W}_{dmd} > \dot{W}^{set}_{supp}, \end{cases}$$

with the production power demand $\dot{W}_{dmd}$, the set point of total power supply $\dot{W}^{set}_{supp}$ and the load gradient k, which is derived from the maximum ramp rate $\max\left|\frac{dj_{avg,E-8}}{dt}\right|$ of the average current density of the stack:

$$k = \frac{A_{cell,E-8}}{2\mathcal{F}u_{E-8}} \max\left|\frac{dj_{avg,E-8}}{dt}\right|,$$

where $A_{cell,E-8}$ represents the total functional surface area of the SOE, $\mathcal{F}$ the Faraday constant and u_{E-8} the steam utilization factor. We select a conservative value of 0.025 A/cm^2 min^{-1} for the maximum ramp rate to avoid thermal damage because of frequent load changes.[44] The production rate of nitrogen is adapted to the hydrogen production rate according to the stoichiometry of the ammonia synthesis reaction. To be noticed, for a sufficiently large load gradient, the deviation between the set point and the real power supply becomes negligible. This assumption is implemented in this work.

For the second purpose, P- and PI-controllers are implemented: the level and pressure control of the steam boiler, the temperature control of the cryogenic distillation column that is responsible for the nitrogen gas quality, the temperature control of the first ammonia synthesis reactor that helps increase the loop stability,[32] and the temperature and flow control of the absorption column of nitric acid that are responsible for the NO_x-emission and the nitric acid quality,

respectively. In this work, all controlled variables are assumed to be measured perfectly. The selection of the controller parameters and the list of the specified variables are presented in the Supporting Information.

4.3 | Optimization problem

The specific production cost C_{prod} per ammonia-equivalent is set as

$$C_{prod} = \frac{C_{capex} + C_{opex}}{\int_T \dot{m}_{prod,NH_3}(t) + 80\% k_{MW} \dot{m}_{prod,HNO_3}(t)},$$

with the time window T, the capital expenditure C_{capex}, the operating expenses C_{opex}, the net ammonia production rate of the production complex $\dot{m}_{prod,NH_3}$, the production rate of nitric acid in the dry mass $\dot{m}_{prod,HNO_3}$ and the conversion ratio k_{MW} from nitric acid to ammonia based on the stoichiometric relationship. k_{MW} is used as an approximation in the cost function only, for the sake of tractability, thanks to the high conversion of the N-atom through the nitric acid production process. The factor 80% in the second term in the denominator is used to underestimate the value of nitric acid production.[40] The capital expenditure includes investments on process equipment as well as the battery. The major part of operating expenses is the power cost. It can be further divided into three parts: the grid power cost, the wind power cost and the additional savings on grid fees through peak load reduction. The export revenue of the unused oxygen and the cooling water cost build the minor part of the operating expenses.

The selection of decision variables depends on the scenario. In the first scenario, the decision variables comprise 15 design parameters and 7 operating parameters. The former consists of the number of SOE cells and the sizes of other process units, while the latter comprises the grid power supply, the pressure levels of the air separation unit and the ammonia synthesis block, and the feeding ratio of upstream (by-)products into the nitric acid production process. In the second scenario, the scaling factor of the wind power supply is optimized in addition to the decision variables in the previous scenario. Beside this, nominal throughputs of compressors and turbines are added for optimization due to variable operating efficiencies. In the last scenario, the decision variable set is expanded by the battery storage size and the charge/discharge power. One hundred and eleven control intervals are used for parameterizing the charge/discharge power with piece-wise constant control profiles. The joint constraints of all scenarios include the process emission constraints on CO_2 and NO_x, and the product quality for intermediate and final products. They also include operational boundaries on temperature and pressure as well as hydrodynamic flow conditions. Only in the third scenario, additional constraints are added to regulate the maximum charging/discharging power flows of the battery storage. Detailed lists of decision variables and constraints are included in the Supporting Information.

The resulting optimization problems are solved with the *NLPSQP* solver.[45] While the optimization problem in the first scenario is time-invariant, the others in the second and third scenario are dynamic optimization problems and are reformulated through a single shooting approach.

5 | RESULTS AND DISCUSSIONS

In this section, we present the optimization results and the results of sensitivity analyses case by case. A short discussion section follows at the end. The most important figures are summarized in Table 1. For the cases in which the plant is operated dynamically, the peak-to-base load ratio is read from the optimized operating profiles and serves as an indicator of the plant's flexibility range. A detailed stream information table for the optimized production complex in the first scenario is provided in the Supporting Information. Stream properties of other cases can be reproduced through the released model.

5.1 | First scenario: Pure grid power supply

Without incorporation of nitric acid production, the power-based ammonia production is not profitable, even if the sales of CO_2 allowances for 13 million \$/year are taken into account. The power-based process reduces primary energy consumption by 12% compared to that of conventional best-available technologies. When incorporating the nitric acid production, the RoI improves by 3 percentage points. This is caused by two factors: first, the capital expenditure on the additional components for nitric acid production is compensated by the cost saving on the SOE, the size of which is decreasing by 30% due to higher power density achieved under the thermal-neutral operation mode; and second, as the SOE is operated at a higher stack temperature around the thermal-neutral point, the energy efficiency is improved. In both process concepts, the heat transfer between the ammonia synthesis and the steam generation is on a similar order, but at a different temperature level because of the difference in operating pressure of the steam boiler. This explains the higher operating pressure of the ammonia synthesis loop in the production complex. Table 2 illustrates the different operating conditions between two process concepts.

The production complex enjoys limited economies of scale under variation of the CO_2 saving target, as shown in Table 3. The main reason is the large share of operating expenses to total costs. Moreover, the most expensive component, the SOE, exhibits a linear cost function of the size.

5.2 | Second scenario: Mixed power supply without deployment of battery

The plant is operated dynamically with a peak-to-base load ratio of 1.7 and absorbs low-cost wind power on a scale of 100 MW. The grid power consumption is reduced by 18% accordingly, which brings in 3 million \$/year of grid fee savings for reduced peak load. The RoI of the production complex reaches 5%. The dynamic operation

TABLE 1 Selected optimization results for different process concepts with a CO_2-reduction equivalent to the emission of a 500 t/d NG-based ammonia production plant

Scenario	First scenario	First scenario	Second scenario	Third scenario	Second scenario
Year	2030	2030	2030	2030	2016
Incorporation of HNO_3 prod.	No	Yes	Yes	Yes	Yes
Spec. prod. cost (\$/t NH_3 eq.)	630	610	580	570	330
Capex (million \$/year)	16	17	23	23	31
Opex (million \$/year)	100	120	100	95	69
Grid fee savings (million \$/year)	–	–	3	5	12
Revenue (million \$/year)	110	130	130	130	120
Revenue distribution (%)					
Chemicals sales	87	89	89	89	99
CO_2 allowance sales	13	11	11	11	1
Return on investment (%)	0	3	5	7	8
Primary energy efficiency[a] (%)	88	86	87[b]	87[b]	129[b]
Grid power (MW)	150	170	140	120	160
Wind power peak (MW)	–	–	95	160	200
Share of wind energy (%)	0	0	22	44	41
NH_3 prod. Rate (t/d)	510	510	510[b]	510[b]	680[b]
HNO_3 prod. Rate (100%wt.t/d)	–	380	330[b]	340[b]	390[b]
SOE cell number (10^6)	17	12	17	17	23
SOE avg. current density (A/m^2)	5,700	9,900	7,200[b]	7,200[b]	6,700[b]
NH_3 synthesis pressure (bar)	140	170	140	160	140
Util. factor ASU by-product (%)	–	100	79	77	50
Util. factor SOE by-product (%)	–	4	20	18	20

Abbreviations: ASU, air separation unit; NG, natural gas; SOC, solid oxide electrolyzer.
[a]The ratio of real primary energy consumption to average energy consumption of best-available technologies (ammonia: 30 GJ/t,[46] nitric acid: −1.6 GJ/t[47]).
[b]Average over time.

deteriorates the energy efficiency slightly. It also leads to an over-dimensioning of the process blocks. The introduction of the dynamic operation shifts the optimum of the operating parameters from its stationary counterpart. For instance, the operating pressure of the ammonia synthesis loop is lower than in the steady-state case. At first sight, it appears to be economically nonfavorable, because the process components in the synthesis loop are significantly over-dimensioned because of the growing circulated gas flow. However, this disadvantage becomes a strength under strong dynamics. Namely, the deterioration of operating efficiency of gas compressors at extreme loads is intentionally exploited to increase power consumption of the ammonia block at the peaks, as shown in Figure 2. More wind power can therefore be integrated and this lowers the operating costs. As a chain effect of the larger synthesis gas flow, the production complex tends to produce less nitric acid, because the synthesis gas releases more heat in the steam boiler and less heat input from the nitric acid plant is needed. Another example that demonstrates the impact of dynamic operation on the selection of the operating parameters is the increasing consumption of the pure oxygen from the SOE and the decreasing absorption of the oxygen-rich by-product from the ASU. This is attributed to different time constants between the unit operations.

The economic performance of the production complex strongly depends on the decarbonization progress of the grid as well as the power price. In the year 2016, the higher carbon footprint of grid power leads to higher production rates to achieve the same emission reduction. Thanks to economies of scale, the marginal capital investment for integrating wind power decreases compared to the year 2030. As a result, the integrated amount of the wind power increases to 200 MW of peak power, which doubles the result of the year 2030. The peak-to-base load ratio becomes 2.3. Thanks to the lower power cost, the specific production cost drops to 330 \$/t and the 8% RoI is the highest value among all scenarios. The revenue from the sales of CO_2 allowances in 2016 is negligible. Moreover, the primary energy consumption is indeed increasing, mainly because of the consumption of nuclear and coal-power from the grid.

5.3 | Third scenario: Mixed power supply with deployment of battery

A battery storage of 140 MWh/70 MW is deployed. The amount of incorporated wind power increases by 70% and accounts for 44% of the total energy consumption. The peak-to-base load ratio increases

from 1.7 in the second scenario to 2.3. The lower power cost because of increased wind power consumption compensates the investment on battery and the specific production cost is slightly reduced. As illustrated in Figure 3a, the load peaks of the production complex are smoothened and extreme operating conditions are avoided. One evidence is the increasing operating pressure of the ammonia synthesis loop. The battery is mainly used for shifting the energy within 2 days, as shown in Figure 3b. This could be a result of the chosen wind power curve. As the daily data are selected with high standard variance, consecutive windless days are not considered.

The optimization result is sensitive to the battery cost. As the cost of battery rises from 200 to 300 $/kWh, the optimal battery size shrinks dramatically to 20 MWh/20 MW. At a cost of 400 $/kWh, which is a conservative cost estimation for the future,[48] deployment of battery is no longer profitable.

TABLE 2 Operating conditions of major process blocks with and without incorporation of HNO_3 production in the first scenario: pure grid power supply

Scenario Incorporation of HNO_3 prod.	First scenario No	First scenario Yes
Steam boiler operating pressure (bar)	2	100
Steam boiler steam outlet temperature (°C)	120	310
SOE avg. current density (A/m^2)	5,700	9,900
SOE stack temperature increase (°C)	100	0
SOE steam inlet temperature (°C)	690	800
NH_3 synthesis pressure (bar)	140	170
NH_3 synthesis outlet temperature (°C)	330	460
NH_3 synthesis conversion of N_2 (–)	0.29	0.21
HNO_3 operating pressure (mono) (bar)	–	9
HNO_3 ammonia burner outlet temperature (°C)	–	880
HNO_3 conversion of N-atom (–)	–	0.97
Heat transfer HE-1 (MWh/ton NH_3 gross)	0.91	0.88
Heat transfer HE-2 (MWh/ton NH_3 gross)	0.35	0.45
Heat transfer HE-3 (MWh/ton NH_3 gross)	0.78	0.67
Heat transfer HE-4 (MWh/ton HNO_3)	–	0.18
Heat transfer HE-5 (MWh/ton HNO_3)	–	0.46
Heat transfer HE-6 (MWh/ton HNO_3)	–	0.31

Abbreviation: SOE, solid oxide electrolyzer.

5.4 | Discussion

In order to stay competitive against conventional productions with an average profit margin of 10%,[49] additional incentives are necessary to improve the RoI of the renewable production complex. In the short term, marketing the load flexibility in the balancing power market may create a further revenue source. Schäfer et al.[5] have demonstrated high economic benefits of this practice on a similarly large energy-intensive process. In the long term, the prospect of the renewable production complex depends on several factors. First, economic

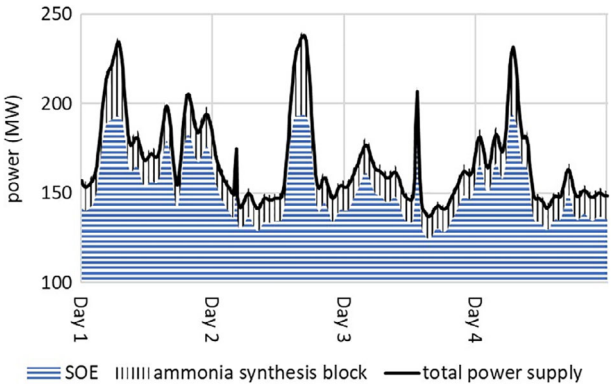

FIGURE 2 Illustration of power consumptions by the SOE and by the ammonia synthesis loop as well as the total power supply in the second scenario: mixed power supply without deployment of battery. SOE, solid oxide electrolyzer [Color figure can be viewed at wileyonlinelibrary.com]

TABLE 3 Production costs of the production complex at different CO_2 saving targets in the first scenario: pure grid power supply

CO_2 saving target (t CO_2/d)	425	850	1,275	1,700
Equation NG-based plant size (t NH_3/d)	250	500	750	1,000
Spec. production cost ($/t)	620	610	610	600
Cost distribution (%)				
Operating expenses	86	88	88	89
Capital expenditure	14	12	12	11
Capital expenditure SOE	6	6	6	6
Return on investment (%)	2.8	3.3	3.7	3.9

Abbreviations: NG, natural gas; SOE, solid oxide electrolyzer.

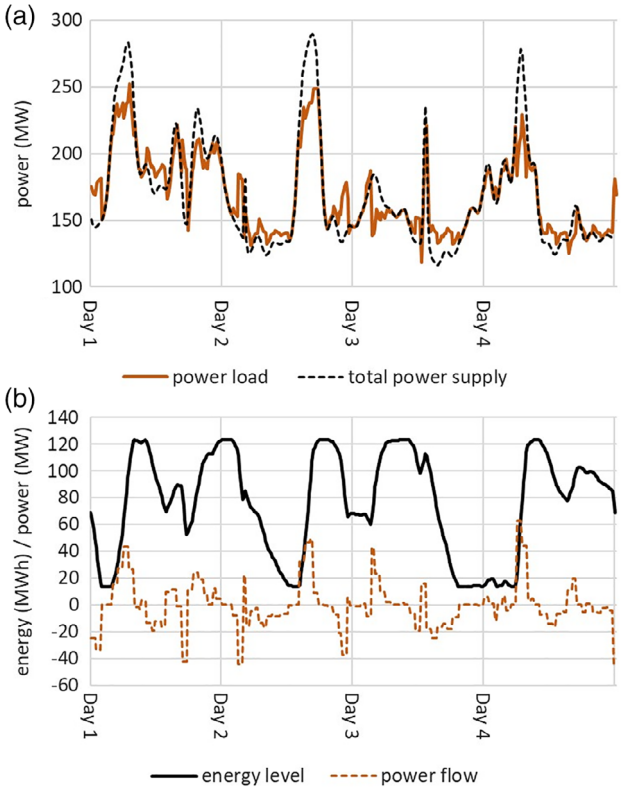

FIGURE 3 Illustration of the operating profiles: (a) the power consumption of the production complex and the total power supply and (b) the amount of energy stored in battery and the charging/discharging power flows in the third scenario: mixed power supply with deployment of battery [Color figure can be viewed at wileyonlinelibrary.com]

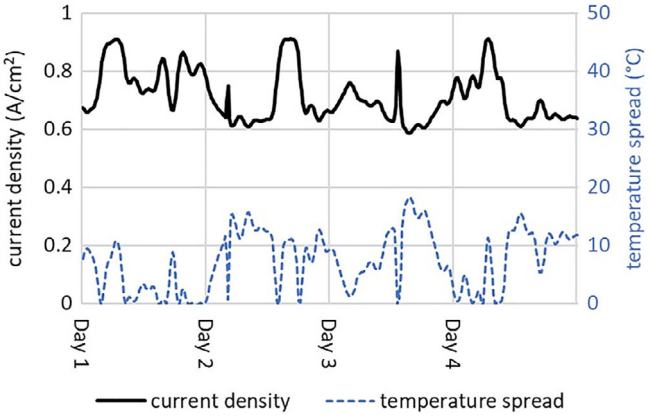

FIGURE 4 Illustration of the average current density over the stack and the temperature spread above the thermal-neutral point in the second scenario: mixed power supply without deployment of battery [Color figure can be viewed at wileyonlinelibrary.com]

incentives for sector coupling need to be designed. As shown in the second scenario, the fast growing electricity cost offsets the revenue from CO_2 allowance sales and hence hampers profitability. A reform of the system of surcharges, fees and taxes is thus crucial.[50] Second, a more strict environmental regulation is required to speed up the technology switch. Allocating full carbon allowances to the domestic ammonia industry is very likely to stifle carbon-free technologies for decades. A gradual cut of the free allowances should be introduced, accompanied by border carbon adjustments that mitigate possible carbon leakages before establishing a global carbon market.[51] Third, technology policies are necessary to promote the carbon-free technology. To become economically competitive, the renewable alternative must double the sales revenue of CO_2 allowances. The resulting carbon price is in accordance with the report of the Carbon Pricing Leadership Coalition[52] to meet the Paris temperature target. Last but not least, closer cooperation between the plant and grid operator is required beyond intensive market interactions. A joint investment and operation of a grid-scale battery storage would increase the utilization of the battery and hence make the battery deployment cheaper, which would be beneficial for the viability of the ammonia plant. While potential plant investors may consult the grid operator to select a site with best opportunities of wind integration and grid supports, the grid planners may acquire a better foresight on the growing load demand through electrification of the chemical processes.

The plant operation in this work has been simplified by assuming a perfect foresight of exogenous inputs, for example, wind availability. In real life, the plant operator needs to exploit economic incentives from the intermittent supply and at the same time meet the demand, while coordinate up- and down-stream processes and manage the inventory in between. To achieve this, we expect three essential technology advances: first, a cross-sector, real-time capable information structure that bridges the production, the management and the external players (e.g., grid), as proposed by Backx et al.[53]; second, tailored models that capture transient behaviors on appropriate time scales of supply and demand, as demonstrated by Schäfer et al.[54]; and third, optimization-based decision tools under uncertainties that are computationally tractable and robust, as reviewed in Dias and Ierapetritou.[55] More open questions and challenges on this topic are reviewed by Daoutidis et al.[56] and Mitsos et al.[7] At the end, it is the plant manager who needs to welcome intentional dynamics and enable the changes.

Besides operation, there are also challenges with respect to process design methods. Based on optimal operation with fixed design, Sass and Mitsos[57] report limitations of quasi-steady operation and underline the importance of applying suitable ramp constraints. In a design optimization problem, it is, however, often difficult to define such realistic ramp constraints a priori. The sizing of the SOE in the second scenario gives a good example: to avoid swings between the endothermic and exothermic operating mode, positive temperature spread over stack is formulated as an operating constraint. Figure 4 shows that the temperature spread drops to zero always at those time points where the current density is under ramping. This transient effect is a result of the interaction between the fast power dynamics inside the SOE stacks and the sluggish temperature dynamics of the peripheries, including the SOE stack itself and the heat exchanger HE-3. The dynamic optimization scheme takes the ramp constraint implicitly into account. Otherwise, the optimal stack size would be underestimated.

6 | CONCLUSION

We proposed a renewable ammonia/nitric acid production complex with comprehensive heat integration measures. We investigated optimal designs in various power supply scenarios with explicit consideration of process dynamics and a simple control scheme. We obtained the following major findings: First, the incorporation of the nitric acid production improves the operating condition of the SOE. The stack utilization increases by 30% and the specific production cost is reduced by 3%. The cost savings become even more significant at a higher stack price in the near future. Second, the proposed plant demonstrates a high degree of operating flexibility under intermittent wind power in-feed. The peak-to-base load ratio reaches 2.3. The flexibility range can be further extended by introducing advanced control methods, which are left to future work. Third, through incorporation of low-cost wind power and deployment of a battery storage the RoI is improved by up to 5 percentage points. However, to become competitive to fossil-based productions, encouraging climate and technology policies are indispensable. Finally, it has been shown that process dynamics plays a crucial role on both design and operation because of transient behaviors, which cannot be captured by time-invariant and even time-variant quasi-stationary models.

The focus of this work is on the analysis of the techno-economic performance of the production complex from a plant owner's perspective. Considering the power intensity and the flexibility demonstrated in this work, it is interesting to investigate the impact of the proposed production complexes with respect to the active participation in energy markets and providing ancillary services. The importance of such production complexes in a 100% renewable energy system is of further interest for studying.

ACKNOWLEDGMENTS

The authors wish to thank the Bosch-Forschungsstiftung for financial support and Dr. Matthias Bitzer for fruitful discussions.

ORCID

Ganzhou Wang https://orcid.org/0000-0002-7856-7723
Alexander Mitsos https://orcid.org/0000-0003-0335-6566
Wolfgang Marquardt https://orcid.org/0000-0002-4455-8378

REFERENCES

1. Lechtenböhmer S, Nilsson LJ, Åhman M, Schneider C. Decarbonising the energy intensive basic materials industry through electrification—implications for future EU electricity demand. *Energy*. 2016;115:1623-1631.
2. Steinberg D, Bielen D, Eichman J, et al. *Electrification and Decarbonization: Exploring US Energy Use and Greenhouse Gas Emissions in Scenarios with Widespread Electrification and Power Sector Decarbonization* [Tech. Rep.]. Golden, CO: National Renewable Energy Lab; 2017. https://www.nrel.gov/docs/fy17osti/68214.pdf. Accessed February 24, 2018.
3. Orella MJ, Roman-Leshkov Y, Brushett FR. Emerging opportunities for electrochemical processing to enable sustainable chemical manufacturing. *Curr Opin Chem Eng*. 2018;20:159-167.
4. Zhang Q, Grossmann IE. Planning and scheduling for industrial demand side management: advances and challenges. *Alternative Energy Sources and Technologies*. Cham: Springer; 2016:383-414.
5. Schäfer P, Westerholt HG, Schweidtmann AM, Ilieva S, Mitsos A. Model-based bidding strategies on the primary balancing market for energy-intense processes. *Comput Chem Eng*. 2018;120:4-14.
6. Baldea M. Employing chemical processes as grid-level energy storage devices. In: Kopanos GM, Liu P, Georgiadis MC, eds. *Advances in Energy Systems Engineering*. Cham: Springer; 2017:247-271.
7. Mitsos A, Asprion N, Floudas CA, et al. Challenges in process optimization for new feedstocks and energy sources. *Comput Chem Eng*. 2018;113:209-221.
8. Appl M. Ammonia. In: Elvers B, ed. *Ullmann's Encyclopedia of Industrial Chemistry*. 2000. https://onlinelibrary.wiley.com/doi/10.1002/14356007.o02_o11.
9. Nørskov J, Chen J, Miranda R, Fitzsimmons T, Stack R. *Sustainable Ammonia Synthesis—Exploring the Scientific Challenges Associated with Discovering Alternative, Sustainable Processes for Ammonia Production* [Tech. Rep.]. U.S. Department of Energy; 2016. https://www.osti.gov/servlets/purl/1283146. Accessed November 20, 2017.
10. Demirhan CD, Tso WW, Powell JB, Pistikopoulos EN. Sustainable ammonia production through process synthesis and global optimization. *AIChE J*. 2018;65(7):e16498.
11. Guillet N, Millet P. Alkaline water electrolysis. In: Godula-Jopek A, ed. *Hydrogen Production: By Electrolysis*. Weinheim: Wiley Online Library; 2015:117-163.
12. Cheema II, Krewer U. Operating envelope of Haber-Bosch process design for power-to-ammonia. *RSC Adv*. 2018;8(61):34926-34936.
13. Reese M, Marquart C, Malmali M, et al. Performance of a small-scale Haber process. *Ind Eng Chem Res*. 2016;55(13):3742-3750.
14. Millet P. PEM water electrolysis. In: Godula-Jopek A, ed. *Hydrogen Production: By Electrolysis*. Weinheim: Wiley Online Library; 2015:63-114.
15. Petipas F, Fu Q, Brisse A, Bouallou C. Transient operation of a solid oxide electrolysis cell. *Int J Hydrogen Energy*. 2013;38(7):2957-2964.
16. Mougin J. Hydrogen production by high-temperature steam electrolysis. *Compendium of Hydrogen Energy*. Cambridge: Elsevier; 2015:225-253.
17. Wang G, Mitsos A, Marquardt W. Conceptual design of ammonia-based energy storage system: system design and time-invariant performance. *AIChE J*. 2017;63(5):1620-1637.
18. Chen C, Lovegrove KM, Sepulveda A, Lavine AS. Design and optimization of an ammonia synthesis system for ammonia-based solar thermochemical energy storage. *Sol Energy*. 2018;159:992-1002.
19. Allman A, Daoutidis P. Optimal scheduling for wind-powered ammonia generation: effects of key design parameters. *Chem Eng Res Des*. 2017;131:5-15.
20. Allman A, Palys MJ, Daoutidis P. Scheduling-informed optimal design of systems with time-varying operation: a wind-powered ammonia case study. *AIChE J*. 2018;65(7):e16434.
21. Du Z, Denkenberger D, Pearce JM. Solar photovoltaic powered on-site ammonia production for nitrogen fertilization. *Sol Energy*. 2015;122:562-568.
22. Allman A, Tiffany D, Kelley S, Daoutidis P. A framework for ammonia supply chain optimization incorporating conventional and renewable generation. *AIChE J*. 2017;63(10):4390-4402.
23. Palys MJ, Allman A, Daoutidis P. Exploring the benefits of modular renewable-powered ammonia production: a supply chain optimization study. *Ind Eng Chem Res*. 2018;58(15):5898-5908.
24. Ghobeity A, Mitsos A. Optimal design and operation of a solar energy receiver and storage. *J Sol Energy Eng*. 2012;134(3):031005.
25. Yuan Z, Chen B, Sin G, Gani R. State-of-the-art and progress in the optimization-based simultaneous design and control for chemical processes. *AIChE J*. 2012;58(6):1640-1659.

26. Chen M, Sun X, Chatzichristodoulou C, Koch S, Hendriksen PV, Mogensen MB. Thermoneutral operation of solid oxide electrolysis cells in potentiostatic mode. *ECS Trans*. 2017;78(1):3077-3088.
27. Chatterjee IB, Joshi JB. Modeling, simulation and optimization: mono pressure nitric acid process. *Chem Eng J*. 2008;138(1–3):556-577.
28. Cao Y, Swartz CLE, Flores-Cerrillo J. Optimal dynamic operation of a high-purity air separation plant under varying market conditions. *Ind Eng Chem Res*. 2016;55(37):9956-9970.
29. Åström K, Bell R. Drum-boiler dynamics. *Automatica*. 2000;36(3):363-378.
30. Udagawa J, Aguiar P, Brandon NP. Hydrogen production through steam electrolysis: model-based steady state performance of a cathode-supported intermediate temperature solid oxide electrolysis cell. *J Power Sources*. 2007;166(1):127-136.
31. Cao Y, Swartz C, Baldea M, Blouin S. Optimization-based assessment of design limitations to air separation plant agility in demand response scenarios. *J Process Control*. 2015;33:37-48.
32. Morud JC, Skogestad S. Analysis of instability in an industrial ammonia reactor. *AIChE J*. 1998;44(4):888-895.
33. Suchak NJ, Jethani KR, Joshi JB. Modeling and simulation of NOx absorption in pilot-scale packed columns. *AIChE J*. 1991;37(3):323-339.
34. Wiegand KW, Scheibler E, Thiemann M. Computation of plate columns for NOx absorption by a new stage-to-stage method. *Chem Eng Technol*. 1990;13(1):289-297.
35. Deutscher Wetterdienst. *Hourly Mean of Station Observations of Wind Speed ca. 10 m Above Ground in m/s, Cuxhaven*; 1969–2016. https://cdc.dwd.de/portal/. Accessed April 22, 2019.
36. UNIDO and IFDC. *Fertilizer Manual*. 3rd ed.; 1998. https://www.unido.org/resources/publications/publications-type/co-published/fertilizer-manual-3rd-edition. Accessed on August 8, 2016
37. Prognos AG, EWI and GWS. *Entwicklung der Energiemärkte—Energiereferenzprognose*; 2014. https://www.bmwi.de/Redaktion/Migration/DE/Downloads/Publikationen/entwicklung-der-energiemaerkte-energiereferenzprognose-kurzfassung.pdf?__blob=publicationFile&v=1. Accessed May 12, 2018.
38. Agora Energiewende. *Future Cost of Onshore Wind—Recent Auction Results, Long-Term Outlook and Implications for Upcoming German Auctions*; 2017. https://www.agora-energiewende.de/fileadmin2/Projekte/2017/Future_Cost_of_Wind/Agora_Future-Cost-of-Wind_WEB.pdf. Accessed June 28, 2018.
39. OCI. OCI N.V. *Trading Update 2017 Q1*; 2017. http://www.oci.nl/media/cms:page_media/62/OCI%20N.V.%20Q1%202017%20Trading%20Report%20Final.pdf. Accessed August 24, 2019.
40. Nielsson FT. *Manual of Fertilizer Processing*. 1st ed. New York: CRC Press; 1986 ISBN 9780824775223.
41. The World Bank. *World Bank Commodities Price Forecast*; 2019. http://pubdocs.worldbank.org/en/598821555973008624/CMO-April-2019-Forecasts.pdf. Accessed August 24, 2019.
42. European Commission. *EU Emissions Trading System* (*EU ETS*); 2019. https://ec.europa.eu/clima/policies/ets/. Accessed August 24, 2019.
43. German Emissions Trading Authority (DEHSt). *Results of Free Allocation of Emission Allowances to Incumbent Installations for the Third Trading Period, 2013-2020*; 2014.
44. Fang Q, Blum L, Menzler N. Performance and degradation of solid oxide electrolysis cells in stack. *J Electrochem Soc*. 2015;162(8):F907-F912.
45. PSE. *gPROMS Optimisation Guide: Release v5.0.1*; 2012.
46. EFMA. *Best Available Techniques for Pollution Prevention and Control in the European Fertilizer Industry—Production of Nitric Acid*; 2000. https://www.fertilizerseurope.com/fileadmin/user_upload/publications/tecnical_publications/BATs/Booklet_2_final.pdf. Accessed November 20, 2018.
47. Wiesenberger H, Kircher J. *State-of-the-Art for the Production of Nitric Acid With Regard to the IPPC Directive*; 2001. https://www.umweltbundesamt.at/fileadmin/site/publikationen/M150.pdf. Accessed November 20, 2018.
48. Ralon P, Taylor M, Ilas A, Diaz-Bone H, Kairies KP. *Electricity Storage and Renewables: Costs and Markets to 2030* [Tech. Rep.]. IRENA; 2017. https://www.irena.org/publications/2017/Oct/Electricity-storage-and-renewables-costs-and-markets. Accessed February 24, 2019.
49. Moya JA, Boulamanti A. *Production Costs From Energy-Intensive Industries in the EU and Third Countries*. Brussels: Publications Office of the European Union; 2016 ISBN 978-92-79-54855-0.
50. BMWi. *Electricity 2030—Long-Term Trends—Tasks for the Coming Years*; 2017. https://www.german-energy-solutions.de/GES/Redaktion/EN/Publications/bmwi/electricity-2030-long-term-trends.pdf. Accessed April 21, 2019.
51. Böhringer C, Rosendahl KE, Storrøsten HB. Robust policies to mitigate carbon leakage. *J Public Econ*. 2017;149:35-46.
52. Carbon Pricing Leadership Coalition. *Report of the High-Level Commission on Carbon Prices*; 2017. https://www.carbonpricingleadership.org/report-of-the-highlevel-commission-on-carbon-prices. Accessed May 12, 2018.
53. Backx T, Bosgra O, Marquardt W. Towards intentional dynamics in supply chain conscious process operations. *Proceedings of Third International Conference on Foundations of Computer-Aided Process Operations*. Vol 5. New York: Elsevier. 1998.
54. Schäfer P, Caspari A, Kleinhans K, Mhamdi A, Mitsos A. Reduced dynamic modeling approach for rectification columns based on compartmentalization and artificial neural networks. *AIChE J*. 2019;65(5):e16568.
55. Dias LS, Ierapetritou MG. Integration of scheduling and control under uncertainties: review and challenges. *Chem Eng Res Des*. 2016;116:98-113.
56. Daoutidis P, Lee JH, Harjunkoski I, Skogestad S, Baldea M, Georgakis C. Integrating operations and control: a perspective and roadmap for future research. *Comput Chem Eng*. 2018;115:179-184.
57. Sass S, Mitsos A. Optimal operation of dynamic (energy) systems: when are quasi-steady models adequate? *Comput Chem Eng*. 2019;124:133-139.

SUPPORTING INFORMATION

Additional supporting information may be found online in the Supporting Information section at the end of this article.

How to cite this article: Wang G, Mitsos A, Marquardt W. Renewable production of ammonia and nitric acid. *AIChE J*. 2020;66:e16947. https://doi.org/10.1002/aic.16947